論文内容の要旨

論文表題　**High-spin Spectroscopy of $^{49-51}$Ti by Fusion Reaction of RI Beam**

(RI ビームの核融合反応による $^{49-51}$Ti の高スピン核分光)

氏　名　　新倉　潤

We have performed in-beam γ-ray spectroscopy via fusion-evaporation reaction of a radio-active (RI) beam to investigate high-spin states in $^{49-51}$Ti.

In neutron-rich Ti isotopes, studies of shell structure are gaining recently much attention from both the experimental and theoretical point of view. The appearance of $N = 32$ and/or 34 sub-shell closures is one of examples of changing the location of single particle orbits in the neutron-rich region. The spectroscopic study at the high-spin yrast states has an advantage to see shell gaps and to test predictions from shell-model calculations, since a single particle states can be arisen in the yrast high-spin states near the closed shell nuclei. In the yrast levels of ^{50}Ti, large gap in the excitation energy of the levels between 7^+ and 6^+ states is corresponded to $N = 28$ shell gap between $\nu f_{7/2}$ and $\nu p_{3/2}$ neutron orbits according to the shell-model calculations. This shell gaps are also predicted neighbor nuclei of ^{50}Ti. We have investigated the yrast high-spin states by in-beam γ-ray spectroscopy in $^{49-51}$Ti.

By means of in-beam γ-ray spectroscopy, the fusion-evaporation reaction is commonly used to populate the high-spin states, since a large amount of angular momentum can be brought into the system. However, nuclei produced by the fusion-evaporation reactions using stable isotope beams are limited, in many cases, to the proton-rich side relative to the β-stability line. A usage of a neutron-rich RI beam allows investigation of the high-spin states in the neutron-rich nuclei. We have developed new method to produce a low-energy RI beam for fusion-evaporation reaction, which called as *secondary fusion reaction*.

Experiment was performed in RIKEN Projectile-fragment spectrometer (RIPS) beam line in RIKEN. The secondary ^{46}Ar beam was produced by the projectile-fragmentation reaction of a ^{48}Ca primary beam on a ^{9}Be target. An aluminum curved degrader installed at momentum focal plane was used to achieve a clear isotope separation and to lower the energy of the beam. Almost pure secondary beam was obtained at second focus (F2) of RIPS. The ^{46}Ar was further lowered in energy using a rotatable aluminum degrader at F2. The intense low-energy RI beam was obtained with An intense low-energy beam with the energy of about 4 MeV/nucleon and with the intensity of 1×10^{8} particle per second was successfully obtained. The low-energy beam transported to final focus (F3), where the secondary target of 9^{9}Be was placed to induce the secondary fusion reaction, $^{9}\mathrm{Be}\left(^{46}\mathrm{Ar}, x\mathrm{n}\right)^{55-x}\mathrm{Ti}$.

Gamma rays emitted from evaporation residues were detected by an array of germanium detectors: Gamma-Ray detector Array with Position and Energy sensitivity (GRAPE) together with two clover and one coaxial detectors placed around the secondary target to cover the angular range between 30° and 130°. The GRAPE provides the position information of the interaction point of detected γ rays by adopted the pulse shape analysis to improve the energy resolution of Doppler-broadened γ rays. The energy resolution after the Doppler correction and the full energy peak efficiency were typically 15 keV and 3.5% for 1.5-keV γ rays.

Data was written in event-by-event bases to disks with trigger condition of two or more germanium detectors firing in coincidence with the beam. A total amount of 1×10^{8} events were collected.

Events associated with the fusion evaporation were identified based on the velocity difference between the beam and the fusion products. By gating relatively low-velocity region in the energy spectrum of the outgoing particles, accidental coincidence background mainly from β-decay of the ^{46}Ar was reduced. Evaporation channel was further separated using a cross-section dependence of the incident beam energy. The energy of ^{46}Ar beam was distributed between 2 and 8 MeV/u at the center of the target due to the energy straggling after passing through the degraders and the beam-line detectors. By gating on different region of the beam energy spectrum, excitation functions of the each γ rays were obtained for indentification of the evaporation channel for each event.

The data analyses were performed by the novel analysis of excitation function analysis, γ-γ coincidence analysis, and multiplicity measurements. High-spin levels up to $(21/2)^{-}$, (11^{+}), and $(17/2)^{-}$ were confirmed for $^{49-51}$Ti, respectively. In left side of Fig. 1, proposed level schemes of $^{49-51}$Ti were shown. The high-spin levels at 7050 keV in ^{49}Ti and at 4406 and 5246 keV in ^{51}Ti are newly identified in the present investigation, respectively.

The shell-model code ANOTINE was used to calculate the energies and wavefunctions of levels in $^{49-51}$Ti within full *pf*-shell model space. The calculation were carried out with four Hamiltonians; FPD6, KB3G, GXPF1 and GXPF1A. Almost all features of the calculated yrast levels are similar with these four Hamiltonians. The results from the shell-model calculation are compared with the experimental level schemes in the right hand side in Fig. 1.

A low-lying levels in ^{50}Ti start with $J^{\pi} = 0^{+}, 2^{+}, 4^{+}, 6^{+}$ sequence and are due to the dominance of the proten $\pi(f_{7/2})^{2}$ multiplet according to the calculation. With a simple interpretation, dominant shell components for low-lying states of ^{49}Ti and ^{51}Ti are regarded as members of the $\pi(f_{7/2})^{2}\nu(f_{7/2})^{7}$ and

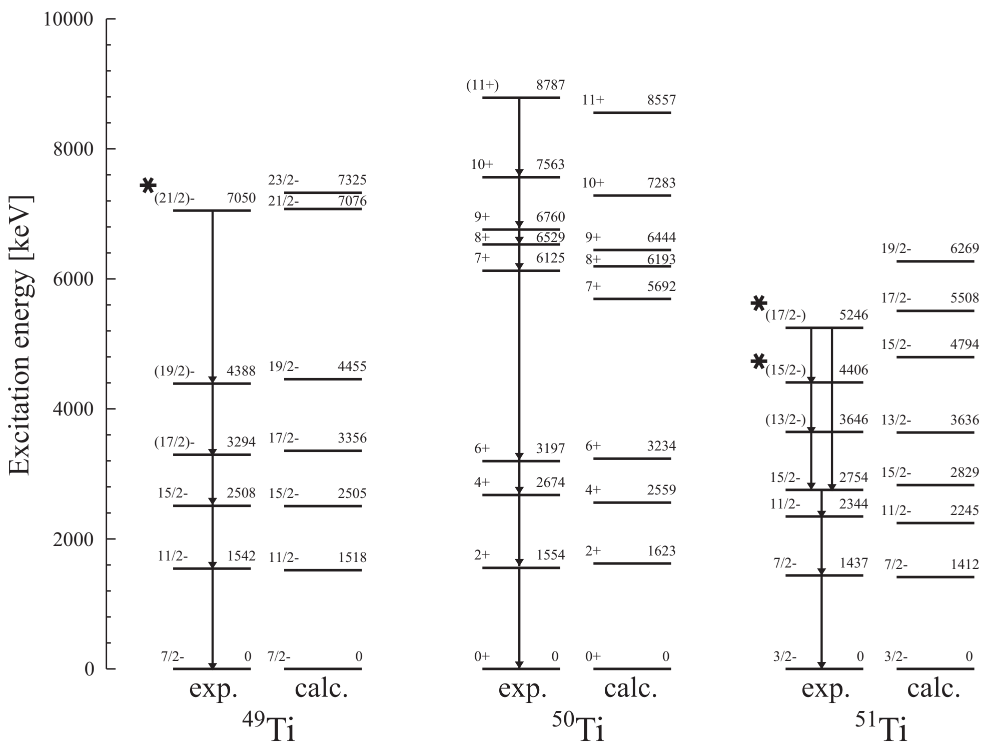

Figure.1: Proposed level schemes for $^{49-51}$Ti obtained in the present experiment (left) and shell-model calculation with GXPF1A effective interaction (right).

$\pi(f_{7/2})^2\nu(f_{7/2})^8(p_{3/2})^1$ multiplet, respectively.

At the high-spin states, $J^\pi = 8^+, 9^+, 10^+, 11^+$ sequence in ^{50}Ti is understood as an one-particle one-hole (1p1h) excitation of the neutron across the N=28 shell gap, $\nu(f_{7/2})^{-1}(p_{3/2})^1$, coupled with the two protons with $J_p = 6^+$ in the $f_{7/2}$ orbit. The newly observed level at 7050 keV in ^{49}Ti, which corresponds to 7076-keV state in the shell-model calculation with GXPF1A, is also considered as the neutron 1p1h configuration, $\pi(f_{7/2})^2\nu(f_{7/2})^6(p_{3/2})^1$. In ^{51}Ti, two high-spin states in ^{51}Ti were observed at 4406 and 5246 keV in the present investigation. The (15/2$^-$) state at 4406 keV, which corresponds to 4876 keV (15/2$^-$) state in the shell-model calculation, is dominated by $\pi(f_{7/2})^2\nu(f_{7/2})^7(p_{3/2})^2$ configuration. Based on the systematic consideration, this level is also dominated by 1p1h configuration of $\nu(f_{7/2})^7(p_{3/2})^1$ as shown of 5865-keV state in the calculation.

In conclusion, we have performed in-beam γ-ray spectroscopy of the high-spin states in $^{49-51}$Ti via the secondary fusion reaction, $^{9}\mathrm{Be}\left(^{46}\mathrm{Ar}, xn\right)^{55-x}\mathrm{Ti}$. The high-spin levels at 7050 keV in ^{49}Ti and at 4406 and 5246 keV in ^{51}Ti are newly identified, respectively. By comparing the full-*pf*-shell calculation, persistency of $N = 28$ shell gap is confirmed in these three nuclei.